

# Increased multidecadal variability of the North Atlantic Oscillation since 1781

NATHALIE F. GOODKIN<sup>1,2\*</sup>, KONRAD A. HUGHEN<sup>1</sup>, SCOTT C. DONEY<sup>1</sup> AND WILLIAM B. CURRY<sup>1</sup>

<sup>1</sup>Woods Hole Oceanographic Institution, Woods Hole, Massachusetts 02543, USA

<sup>2</sup>University of Hong Kong, Pokfulam Road, Hong Kong SAR

\*e-mail: goodkin@hku.hk

Published online: 9 November 2008; doi:10.1038/ngeo352

The North Atlantic Oscillation is a meridional oscillation of atmospheric mass measured between Iceland and the Açores<sup>1,2</sup>, which drives winter climate variability in eastern North America and Europe. A prolonged period of the positive phase during the 1990s led to the suggestion that anthropogenic warming was affecting the behaviour of the North Atlantic Oscillation<sup>3,4</sup>. However, instrumental records<sup>1,5</sup> are too short to compare observations during periods of extended warm and cold hemispheric temperatures, and existing palaeoclimate reconstructions<sup>6,7</sup> primarily capture terrestrial variability. Here we present a record of Sr/Ca, a sea surface temperature proxy, from a Bermuda coral from 1781 to 1999. We use this monthly resolved record to reconstruct past variability of the North Atlantic Oscillation at multiple frequencies. Our record shows enhanced multidecadal scale variability during the late twentieth century compared with the end of the Little Ice Age (1800–1850). We suggest that variability within the North Atlantic Oscillation is linked to the mean temperature of the Northern Hemisphere, which must be considered in any long-term predictions.

The North Atlantic Oscillation (NAO) is the dominant mode of winter pressure variability over the North Atlantic<sup>8</sup>. In a positive NAO index (NAOI), both the low-pressure zone over Iceland (65° N, 23° W) and the high-pressure zone over the Açores (38° N, 26° W) are intensified, resulting in changes in the strength, incidence and pathway of winter storms crossing the Atlantic<sup>9</sup>. The NAO's climatic influence extends from the eastern United States to western Europe<sup>2</sup>, impacting human activities such as shipping, oil drilling, fisheries, hydroelectric power generation and coastal management (for example refs 2,10). Improving our ability to predict shifts in the phase and intensity of the NAO is therefore a prerequisite to mitigating the economic impacts of future climate change<sup>11,12</sup>.

Beginning in the early 1950s, the North Atlantic region experienced extended periods of intense negative and positive NAOI that are unprecedented in the instrumental record (Fig. 1a)<sup>1</sup>. Hypotheses link the anomalous period of positive NAOI between 1970 and 2000 to anthropogenic warming<sup>3,4</sup>. However, short instrumental observations do not constrain long-term multidecadal NAO behaviour or identify links between NAO behaviour and mean climate with confidence<sup>6,13</sup>. One approach to reconstructing NAO variability beyond the instrumental record has been the use of tree-ring chronologies combined with ice cores and historical climate data to capture the terrestrial teleconnections adjacent to the Atlantic basin<sup>6,7</sup>.

Terrestrial data, however, do not fully capture oceanic processes linked to NAO variability. Sea surface temperatures (SSTs) from

the North Atlantic basin correlate with NAO signals at both interannual and multidecadal scales<sup>14</sup>, but short instrumental records from relatively few locations limit our understanding of ocean–atmosphere dynamics with regard to the NAO. One multicentury marine record of the NAO has been constructed on the basis of the relation of mollusc growth rates to mixed layer depth<sup>15</sup> in Scandinavia. However, additional century-scale observations of NAO variability from marine archives are needed during intervals of different mean climate in order to understand NAO variability within the critical North Atlantic basin. Here we present an SST-based, multifrequency reconstruction of the NAO, extending back to the end of the Little Ice Age (LIA). It is the first non-terrestrial reconstruction showing long-term multidecadal behaviour of the NAO (see Supplementary Information, Fig. S1) located within the NAO ‘centre of action’ in the western Atlantic. This NAO record is statistically evaluated for long-term variability in amplitude and phase, and for whether changes in behaviour correlate to the shift from cool to warm hemispheric conditions between the end of the LIA and the late twentieth century (Fig. 1c).

Winter SST and coral Sr/Ca at Bermuda have been shown to correlate with the NAO index on inter-annual and multidecadal frequencies (with positive and negative correlation, respectively)<sup>16–19</sup>. Changing latitudinal wind patterns associated with the NAO alter large-scale Ekman pumping and surface heat flux, leading to a positive NAO–positive SST relationship on interannual timescales<sup>16</sup>. On multidecadal timescales, SST has an inverse relationship with the NAO at Bermuda. Though less well understood, this effect is believed to result from both advection of the interannual signal<sup>20–22</sup>, which is inverse in much of the Atlantic beyond Bermuda, and changes in large-scale ocean circulation, including meridional overturning circulation and Labrador Sea convection<sup>16,17</sup>.

A 218-year-long record of the NAO was constructed from winter coral strontium-to-calcium ratio, a proxy for winter SST (refs 6,23) (Fig. 1b). Cross-spectral analysis compared the negative of coral winter Sr/Ca to an NAO record from 1864 to 1999 on the basis of instrumental data<sup>1</sup> (Fig. 2a) (see the Methods section for details of statistical treatments). The comparisons show significant coherence over two frequency intervals, periodicities greater than 15 years and periodicities between ~3 and 5 years (Fig. 2). At multidecadal frequencies the negative of coral winter Sr/Ca and NAO records are antiphase, whereas at inter-annual frequencies they are in phase (Fig. 2b). The phase relationships of coral Sr/Ca to the NAO record in these two frequency bands are consistent with SST-NAO analyses from instrumental data and

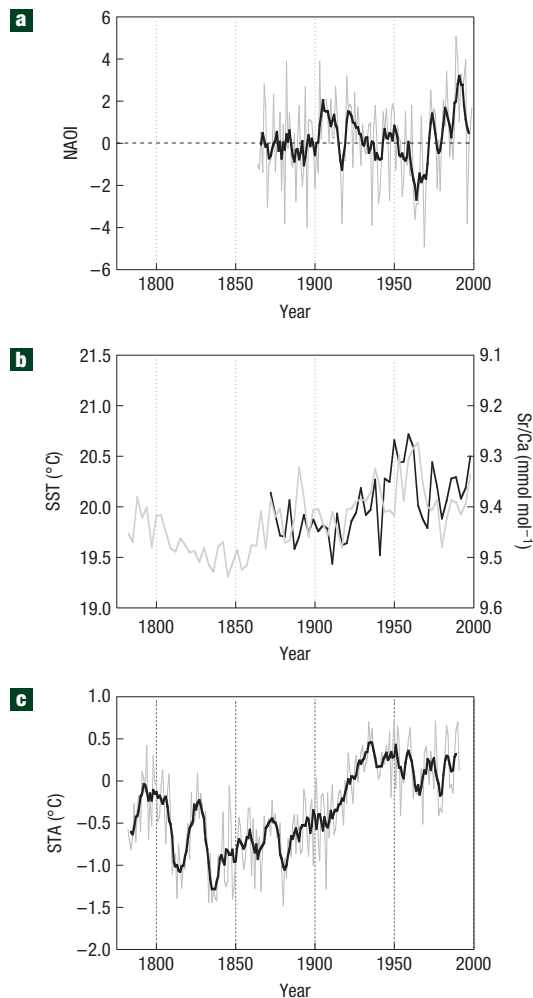


**Figure 1** Climate records from the North Atlantic region. **a**, Instrumental record of the NAO (ref. 1) annually (grey) and 5 year running mean (black). **b**, Three year averaged coral winter SST from Sr/Ca (grey) and instrumental data (black) (HadISST (ref. 35)) versus time. Three year averages are shown, as this is the shortest time period of coherence between the winter coral Sr/Ca and the instrumental NAO. A significant coherence ( $>95\%$ ) is found between the winter coral Sr/Ca and SST ( $r=0.44$ ,  $p=0.0030$ ,  $n=43$ ). **c**, A multiproxy record of Northern Hemisphere surface temperature anomalies<sup>24</sup>—annually (grey) and 5 year running mean (black).

model results<sup>16,17,20</sup> (Fig. 2b). The coral does not capture known NAO variability in 7–10 year periods (Fig. 2c). Although the reason is not understood, one possibility is the shift between the in-phase and antiphase relationship.

Coral Sr/Ca reflects a broad spectrum of SST changes, but not all SST variability at Bermuda is driven by the NAO. At low frequencies ( $<0.1$  cycles per year), the coral winter Sr/Ca record shows significant coherence with both the NAO and northern hemisphere average surface temperature (JSTA)<sup>24</sup>. The strongest agreement between the Sr/Ca and JSTA records is due to generally increasing trends from the earliest part of the records to today (Fig. 1b,c). However, if the winter Sr/Ca and JSTA records are each linearly detrended (from 1781 to 1999) before cross-correlation analysis, then the low-frequency coherence is considerably smaller and not statistically significant (see Supplementary Information, Fig. S2). In addition, the instrumental NAO and JSTA records have

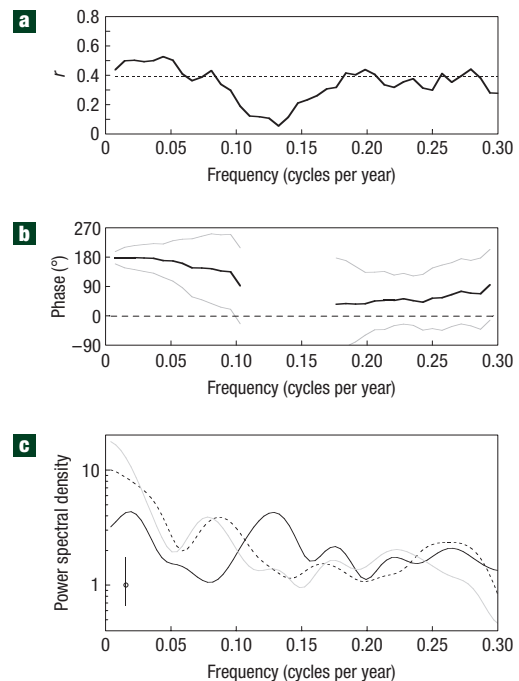


**Figure 2** Spectral analysis of regional records. **a**, The spectral coherence ( $r$ ) (solid) between the negative of the winter Sr/Ca and the NAO instrumental records, including the 95% confidence (dashed), from 1864 to 1999 (the full length of the NAO record). **b**, The phase relationship between the Sr/Ca and NAOI records (solid black), including error calculation (solid grey), surrounding periods of significant coherence. **c**, Spectral results of the NAOI (solid black), SST (solid grey) and Sr/Ca (dashed) from 1871 to 1999, the duration of HadISST, which is the shortest record. The error bar represents 90% confidence.

no significant correlation at frequencies less than 0.08 cycles per year. While temperature seems to be gradually increasing from 1864 to 1999, the NAO does not show a similar secular trend (Fig. 1, Supplementary Information, Fig. S2). We therefore apply a 20–100 year band-pass filter to remove the very low-frequency ( $<0.01$  cycles per year) trend in the Sr/Ca record, which seems to reflect hemispheric mean temperature and is probably dominated by climate processes other than the NAO, such as solar variability and anthropogenic warming<sup>25</sup>.

On the basis of these results, coral Sr/Ca was used to reconstruct the NAO (Fig. 3a) by filtering the Sr/Ca record to isolate the two frequency bands where the coral data are coherent with the NAO. To evaluate this approach, the same process was applied to instrumental SST and NAO data; the 3–5 year coherence is 0.40 (95% significant,  $n_{\text{effective}}=124$ ) and the 20–100 year coherence is  $-0.47$  (95% significant,  $n_{\text{effective}}=24$ ), both with the expected phase relationship. These results agree well with those found for the Sr/Ca and instrumental NAO (Fig. 2a,b, Table 1).

To compare NAO behaviour back through time, 3–5 year and 20–100 year filters were also applied to NAO records from both instrumental sea-level pressure data<sup>1</sup> and a compilation of instrumental pressure, temperature and precipitation data primarily from Europe<sup>7</sup> (Fig. 3). The maximum lagged ( $\pm 1$  year) correlations of the interannual (3–5 year band) coral Sr/Ca NAO reconstruction to the NAO proxy record<sup>7</sup> show minimal differences between the warmest period of the twentieth century (1950–1997) and the end of the LIA (1800–1849) (Table 1). In addition, the mean variance of the interannual Sr/Ca NAO record does not

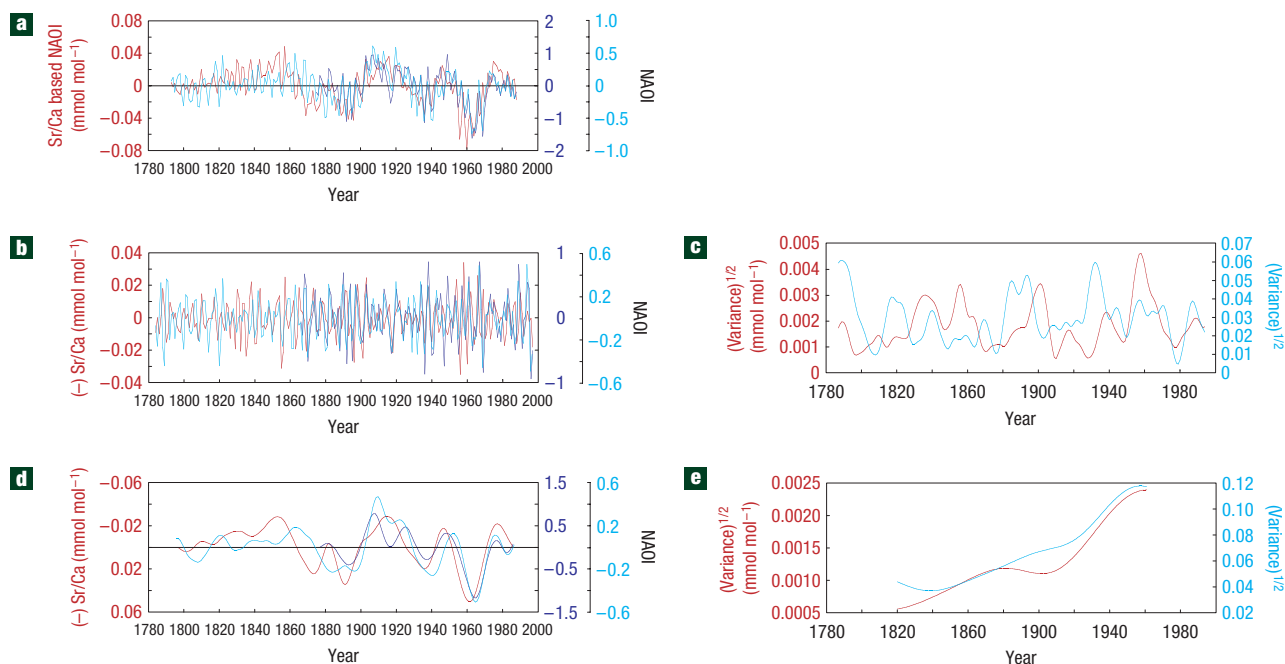


**Figure 3** NAOI records and wavelet analysis. **a**, Records of the NAOI combining periodicities of 20–100 years and 3–5 years from coral Sr/Ca (red), instrumental<sup>1</sup> (dark blue) and terrestrial<sup>7</sup> (light blue) data. **b**, 3–5 year band-pass filter of Sr/Ca, instrumental and terrestrial data. **c**, Square root of the variance in spectral power over a 3–5 year frequency band for coral Sr/Ca and for terrestrial data. **d**, 20–100 year band-pass filter of Sr/Ca, instrumental and terrestrial data. **e**, Square root of the variance in spectral power over a 20–50 year frequency band for coral Sr/Ca and for terrestrial data<sup>7</sup>.

**Table 1** Correlation ( $r$ ) between the negative of the winter coral Sr/Ca and instrumental and proxy records of the NAO.

	Instrumental and proxy records	
	Hurrell	Luterbacher
Inter-annual (3–5 year) correlations ( $r$ )		
1950–1996	0.48*	0.36*
1800–1849		0.29*
Multidecadal (20–100 year) correlations ( $r$ )		
1875–1985 <sup>‡</sup>	–0.76*	–0.77*
1950–1985	–0.82*	–0.79 <sup>†</sup>
1800–1849		–0.49

\*95% significant.

<sup>†</sup>90% significant, with  $n$  adjusted for auto-covariance due to filtering.

<sup>‡</sup>Correlation of maximum overlap of the three records. Interannual correlations are maximum lagged correlations ( $\pm 1$  year).

differ between the two time periods within statistical significance (variance 1948–1997 = 0.00017, variance 1800–1849 = 0.00011,  $F$ -test statistic  $F = 1.6$ , 95%,  $n_{\text{effective}} = 49$ ).

In the multidecadal (20–100 year) frequency band, the Sr/Ca NAO shows a strong correlation to the instrumental and proxy NAO records (Table 1). Separating the records into the beginning of the nineteenth century (1800–1849) and the end of the twentieth century (1936–1985) shows that, during times of warm hemispheric mean temperatures (Fig. 1c), the coral record has a stronger coherence with the terrestrial proxy NAO record ( $r = -0.80$  warm,  $r = -0.49$  cold) (Table 1). Age model bias in either reconstruction is expected to be less than 15 years, and is unlikely to explain the change in coherence of the marine and terrestrial records (Table 1). A change in stationarity of the NAO spatial pattern could result in reduced correlations between

terrestrial and marine NAO records during the LIA, or lead to increased influence of other local climate systems. However, such changes would need to occur in both marine and terrestrial regions to explain the two consistent NAO records.

Simultaneous to the reduction in multidecadal coherence is a significant reduction in variance during intervals of colder hemispheric temperature relative to warmer temperatures (variance 1800–1849 =  $5.1 \times 10^{-5}$ , variance 1936–1985 =  $55 \times 10^{-5}$ ,  $F = 10.7$ , 95% significant,  $n_{\text{effective}} = 9$ ). A similar result was noted in a reconstruction based primarily on tree rings<sup>6</sup>, but the lack of a low-frequency variability in the proxy record (see Supplementary Information, Fig. S1) makes the comparison of multidecadal trends between the LIA and the twentieth century uncertain.

To illustrate this change in variance, wavelet analysis of the unfiltered coral winter Sr/Ca (marine) and Luterbacher *et al.*<sup>7</sup> (terrestrial) NAO records, using a Morlet basis function<sup>26</sup>, was carried out at 3–5 year and 20–50 year periodicities. In the 3–5 year frequency band, intervals of elevated spectral power are observed during both warm and cool periods. This result is consistent with amplitude variance results presented previously. The multidecadal power is not equally distributed through time and seems to be tied to hemispheric temperatures (Fig. 3c). The spectral power in both independent records is greatest during the warmest part of the record (1920–1960), and weakest during the earlier cooler interval. This result is consistent with the amplitude variance results and is clearly visible in the records themselves (Fig. 3a,d). The increase in multidecadal NAO variability suggests an influence of anthropogenic warming that occurs simultaneously with a stronger ocean–atmosphere connection. Reduced low-frequency variance in the NAO, and subsequent decreased signal-to-noise ratio in both marine and terrestrial NAO reconstructions remains the most likely explanation for the reduced correlation between NAO records during the LIA (Table 1).

The new coral Sr/Ca marine record shows that at multidecadal frequencies NAO behaviour is correlated to shifts in hemispheric mean temperature, with greatly increasing power in both marine and atmospheric NAO records with increasing temperatures (Fig. 3). Intervals of both positive- and negative-phase NAO occur both during the LIA and the late twentieth century. Anthropogenic warming does not therefore seem to be altering whether the NAOI is positive or negative at multidecadal timescales, but rather it seems to be acting to increase NAO multidecadal variability, suggesting that prolonged intervals of extreme positive and negative NAO index will probably continue if temperatures continue to rise.

Internationally, climate modelling groups are investing significant effort to develop regional climate forecasts for the next several decades for applications such as climate adaptation<sup>27</sup>. Elevated multidecadal variance of the NAO relative to historical knowledge could complicate these efforts and result in a decrease in climate predictability for the North Atlantic Basin over the next several decades. Because the transitions between extended periods of more strongly positive or negative NAO index are currently difficult to forecast, the resulting climate anomalies may overwhelm the more gradual (and perhaps more predictable) anthropogenic climate trends on these timescales. However, a broad distribution of marine records could advance our knowledge of NAO–SST linkages at the multidecadal scale, and, together with the long timescales of decadal SST trends, serve to improve future projections of the state of the NAO.

## METHODS

A brain coral (*Diploria labyrinthiformis*) was collected live in May 2000 from the southeastern edge of the Bermuda platform (64° W, 32° N) at 16 m depth.

The coral NAO proxy is based on the inverse relationship between winter (December–March) coral Sr/Ca and winter SST (refs 6,23) (Fig. 1b), which has been shown to have no interannual growth-rate influences<sup>25,28</sup>.

X-radiographs of 5-mm-thick slabs cut along the axis of maximum growth of the brain coral reveal well-defined seasonal (summer–winter) growth bands. Using the x-radiographs as a guide, samples were drilled down the length of the solid septotheca (calyx wall) at 0.33 mm intervals to achieve approximately monthly resolution from 1781 to 1999. Sr and Ca were measured simultaneously on an inductively coupled plasma atomic emission spectrometer at Woods Hole Oceanographic Institution. Materials and methods can be found in greater detail in previous publications<sup>25,28</sup>.

Density banding from X-rays was used to construct an annual age model that was refined by maximizing the correlation of monthly Sr/Ca to monthly averaged SSTs measured at nearby ocean Hydrostation S. Beyond the instrumental record, months were assigned by correlating Sr/Ca to an average seasonal climatology of the Hydrostation S data. The coral data were then re-sampled at evenly spaced monthly intervals to identify winter months. Some age model error is anticipated owing to noise in the Sr/Ca record and in the X-ray images of the annual bands, which could serve to either add or eliminate years inappropriately. However, it is more likely that the coral age model will be biased because of missing years (bands), resulting from years of little or no growth. This bias is likely to reach a maximum between 1830 and 1865, when growth rates were lowest<sup>25</sup>.

Cross-spectral analysis comparing the negative of the winter Sr/Ca record to the other instrumental and proxy NAO records is completed using a non-parametric multitaper method<sup>29–32</sup>. Results of this method are shown in Fig. 2a,b and Supplementary Information, Fig. S2. Unless specified (see caption Supplementary Information, Fig. S2), the records are not detrended or prewhitened before analysis. We used ten windows for the multitaper method. 95% confidence is tabulated from a Gaussian process<sup>33</sup> using degrees of freedom estimated from the number of windows (NW) used in the multitaper method from the following equation:

$$\text{degrees of freedom} = \text{NW}^2 - 1.$$

Error estimates on phase relationships were generated using a Monte Carlo simulation in which 50 probable and accurate realizations were generated from stationary white-noise processes.

Records of the NAO at the pertinent frequencies were then generated with Hanning window band-pass filters selecting frequencies between 3 and 5 years per cycle and 20 and 100 years per cycle. The two filtered time-series were then combined by addition for the NAO instrumental record and the instrumental and terrestrial-based proxy record. In the case of the Sr/Ca record, the 20–100 year frequency band (antiphase to the instrumental NAO record) was inverted before adding to the 3–5 year band.

The length of the multidecadal record was maximized by shortening the Hanning window on each end of the record. In order to maintain the validity of the record, the shortest window used was a 20–30 year filter on either end. This shortens the original record by a total of 28 years, losing 14 years at both the start and the end of the reconstruction.

Significance levels used to evaluate the coherence results in Table 1 and in variance analysis carried out on the band-pass-filtered records presented in the text were calculated on the basis of an effective number of degrees of freedom that took into account the covariance due to the band-pass filters. This was carried out by calculating the auto-covariance from the zero lag to the first zero crossing described in ref. 34 (pp. 261–263).

Spectral analysis shown in Fig. 2c and Supplementary Information, Fig. S1 was generated using Hamming windows with 50% overlap. The analysis was carried out after subtracting the mean from each record to centre the values on zero and then dividing by the standard deviation to normalize variance. The length of the records corresponded to that of the shortest record in the comparison, so that each record is examined over the same time period. Data in Fig. 2c were truncated from 129 to 128 data points and had five overlapping windows. Data in Supplementary Information, Fig. S1 were padded with zeros to 256 data points (from 140) and thus had 11 overlapping windows. The error bar shown represents 90% confidence.

Wavelet analysis shown in Fig. 3 was carried out on the winter-time Sr/Ca and terrestrial proxy record, using a Morlet basis function, following previously published methods<sup>26</sup>. Neither record was treated in any way before analysis. The multidecadal variance band was extended only to 50 year periodicities to enable investigation of the multidecadal power within the confidence limits of the analysis.

Received 14 July 2008; accepted 10 October 2008; published 9 November 2008.

## References

- Hurrell, J. W. Decadal trends in the north Atlantic oscillation—regional temperatures and precipitation. *Science* **269**, 676–679 (1995).
- Hurrell, J., Kushnir, Y., Ottersen, G. & Visbeck, M. in *The North Atlantic Oscillation: Climatic Significance and Environmental Impact* (eds Hurrell, J., Kushnir, Y., Ottersen, G. & Visbeck, M.) 1–36 (American Geophysical Union, 2003).
- Shindell, D. T., Miller, R. L., Schmidt, G. & Pandolfo, L. Simulation of recent northern winter climate trends by greenhouse-gas forcing. *Nature* **399**, 452–455 (1999).
- Hurrell, J. W. Influence of variations in extratropical wintertime teleconnections on Northern Hemisphere temperature. *Geophys. Res. Lett.* **23**, 665–668 (1996).
- Jones, P. D., Jonsson, T. & Wheeler, D. Extension to the North Atlantic Oscillation using early instrumental pressure observations from Gibraltar and south-west Iceland. *Int. J. Climatol.* **17**, 1433–1450 (1997).
- Cook, E. R., D'Arrigo, R. D. & Mann, M. E. A well-verified, multiproxy reconstruction of the winter North Atlantic Oscillation index since AD 1400. *J. Clim.* **15**, 1754–1764 (2002).
- Luterbacher, J. *et al.* Extending the North Atlantic Oscillation reconstructions back to 1500. *Atmos. Sci. Lett.* **2**, 114–124 (2001).
- Jones, P. D., Osborn, T. J. & Briffa, K. R. in *The North Atlantic Oscillation: Climatic Significance and Environmental Impact* (eds Hurrell, J., Kushnir, Y., Ottersen, G. & Visbeck, M.) (American Geophysical Union, 2003).
- Ruprecht, E., Schroeder, S. & Ubl, S. On the relation between NAO and water vapour transport towards Europe. *Meteorologische Zeitschrift* **11**, 395–401 (2002).
- Kushnir, Y., Cardone, V. J., Greenwood, J. G. & Cane, M. A. The recent increase in North Atlantic wave heights. *J. Clim.* **10**, 2107–2113 (1997).
- Hurrell, J. W., Kushnir, Y. & Visbeck, M. Climate—The North Atlantic Oscillation. *Science* **291**, 603–605 (2001).
- Rodwell, M. J. in *The North Atlantic Oscillation: Climatic Significance and Environmental Impact* (eds Hurrell, J., Kushnir, Y., Ottersen, G. & Visbeck, M.) 173–192 (American Geophysical Union, 2003).
- Joyce, T. M. One hundred plus years of wintertime climate variability in the Eastern United States. *J. Clim.* **15**, 1076–1086 (2002).
- Czaja, A. & Frankignoul, C. Observed impact of Atlantic SST anomalies on the North Atlantic oscillation. *J. Clim.* **15**, 606–623 (2002).
- Schoene, B. R. *et al.* North Atlantic Oscillation dynamics recorded in shells of a long-lived bivalve mollusk. *Geology* **31**, 1037–1040 (2003).
- Visbeck, M. *et al.* in *The North Atlantic Oscillation: Climate Significance and Environmental Impact* (eds Hurrell, J., Kushnir, Y., Ottersen, G. & Visbeck, M.) 113–145 (American Geophysical Union, 2003).
- Eden, C. & Willebrand, J. Mechanisms of interannual to decadal variability of the North Atlantic circulation. *J. Clim.* **14**, 2266–2280 (2001).
- Cohen, A. L., Smith, S. R., McCartney, M. S. & van Etten, J. How brain corals record climate: An integration of skeletal structure, growth and chemistry of *Diploria labyrinthiformis* from Bermuda. *Mar. Ecol.-Prog. Ser.* **271**, 147–158 (2004).
- Kuhnert, H., Cruger, T. & Patzold, J. NAO signature in a Bermuda coral Sr/Ca record. *Geochim. Geophys. Geosyst.* **6**, Q04004 (2005).

20. Krahnmann, G., Visbeck, M. & Reverdin, G. Formation and propagation of temperature anomalies along the North Atlantic Current. *J. Phys. Oceanogr.* **31**, 1287–1303 (2001).
21. Visbeck, M., Cullen, H., Krahnmann, G. & Naik, N. An oceans model's response to North Atlantic Oscillation like wind forcing. *Geophys. Res. Lett.* **25**, 4521–4524 (1998).
22. Marshall, J. *et al.* North Atlantic climate variability: Phenomena, impacts and mechanisms. *Int. J. Climatol.* **21**, 1863–1898 (2001).
23. Smith, S. V., Buddemeier, R. W., Redalje, R. C. & Houck, J. E. Strontium–calcium thermometry in coral skeletons. *Science* **204**, 404–407 (1979).
24. Jones, P. D., Briffa, K. R., Barnett, T. P. & Tett, S. F. B. High-resolution palaeoclimatic records for the last millennium: Interpretation, integration and comparison with general circulation model control-run temperatures. *Holocene* **8**, 455–471 (1998).
25. Goodkin, N. F., Hughen, K. A., Curry, W. B. & Ostermann, D. R. Sea surface temperature and salinity variability at Bermuda during the end of the little ice age. *Paleoceanography* **23**, PA3203 (2008).
26. Torrence, C. & Compo, G. P. A practical guide to wavelet analysis. *Bull. Am. Meteorol. Soc.* **79**, 61–78 (1998).
27. IPCC. Climate Change 2007: The Fourth Assessment Report of the Intergovernmental Panel on Climate Change (Cambridge Univ. Press, 2007).
28. Goodkin, N. F., Hughen, K., Cohen, A. C. & Smith, S. R. Record of little ice age sea surface temperatures at Bermuda using a growth-dependent calibration of coral Sr/Ca. *Paleoceanography* **20**, PA4016 (2005).
29. Huybers, P. <<http://www.people.fas.harvard.edu/~phuybers/Mfiles/index.html>> (2003).
30. Huybers, P. & Denton, G. Antarctic temperature at orbital timescales controlled by local summer duration. *Nature Geosci.* (2008, in the press).
31. Thomson, D. J. Time series analysis of Holocene climate data. *Phil. Trans. R. Soc. Lond. A* **330**, 601–616 (1990).
32. Percival, D. & Walden, A. *Spectral Analysis for Physical Applications* (Cambridge Univ. Press, 1993).
33. Amos, D. & Koopmans, L. *Tables of Distribution of the Coefficient of Coherence for Stationary Bivariate Gaussian Processes* (Sandia Corp., 1963).
34. Emery, W. J. & Thompson, R. E. *Data Analysis Methods in Physical Oceanography* (Elsevier, 1998).
35. Rayner, N. A. *et al.* Global analyses of sea surface temperature, sea ice, and night marine air temperature since the late nineteenth century. *J. Geophys. Res.* **108**, 4407 (2003).

Supplementary Information accompanies the paper at [www.nature.com/naturegeoscience](http://www.nature.com/naturegeoscience).

#### Acknowledgements

We are indebted to A. Cohen for providing the coral samples and to M. McCartney. This analysis benefited greatly from the comments of P. Huybers and T. Farrar. Thanks to E. Boyle, A. Czaja, A. Solow, D. Ostermann, S. Smith, G. Webster, S. du Putron, G. Piniak, J. Pitt, D. Schrag, C. Bertrand, P. Landry, and D. Glover for informative conversations, technical and logistical help. A Woods Hole Oceanographic Institution OCCI Fellowship, and grants from NSF (OCE-0402728) and Woods Hole Oceanographic Institution supported this work.

#### Author information

Reprints and permissions information is available online at <http://npg.nature.com/reprintsandpermissions>. Correspondence and requests for materials should be addressed to N.F.G.